International Journal of Bifurcation and Chaos, Vol. 20, No. 4 (2010) 1185–1191

DOI: 10.1142/S0218127410026381

NEW CHARACTERISTIC RELATIONS IN TYPE-II INTERMITTENCY

EZEQUIEL DEL RIO
Dpto. Fisica Aplicada, ETSI Aeronauticos,
Universidad Politecnica de Madrid, 28040 Madrid, Spain
ezequiel.delrio@upm.es

SERGIO ELASKAR
Dpto. de Aeronautica, Facultad de Ciencias Exactas,
Fisicas y Naturales, Universidad Nacional de Cordoba,
Avenida Velez Sarfield, 1611. 5000 Cordoba, Argentina
selaskar@efn.uncor.edu

Received August 5, 2009; Revised August 18, 2009

We study analytically and numerically the reinjection probability density for type-II intermittency. We find a new one-parameter class of reinjection probability density where the classical uniform reinjection is a particular case. We derive a new duration probability density of the laminar phase. New characteristic relations $e^{\beta}(-1 < \beta < 0)$ appear where the exponet β deepens on the reinjection probability distributions. Analytical results are in agreement with the numerical simulations.

Keywords: Intermittency; characteristic relations; tent map.

1. Introduction

Intermittency is a particular form of deterministic chaos, in which transitions between different behaviors of the system occur. In a crisis-induced intermittency the transitions take place between chaotic attractors [Grebogi *et al.*, 1987; Ott, 1993]. In the Pomeau and Manneville intermittency, transitions between laminar and chaotic phases occur. A system is in a regular behavior until, with a small change in a parameter, it begins to show chaotic burst at irregular intervals [Ott, 1993]. Pomeau and Manneville introduced this intermittency concept related to the Lorenz system [Manneville & Pomeau, 1979; Pomeau & Manneville, 1980]. Intermittency has been studied in many experiments, associated with Benard convection [Dubois *et al.*, 1983], electronic circuits [Del Rio *et al.*, 1994; Stavrinides *et al.*, 2008] or human heart [Zebrowski & Baranowski, 2004], for instance.

Type-II intermittency is one of the three intermittencies proposed by Pomeau and Manneville, being in a subcritical Hopf bifurcation. The reinjection mechanism into laminar region is dependent on the chaotic phase behavior, so it is a global property, and this was reported as an important factor in the scaling relation of the laminar length [Crutchfield *et al.*, 1982; Kim *et al.*, 1994; Kim *et al.*, 1998]. Hence the probability density of reinjection (PRD) of the system back from chaotic burst into the laminar zone is determined by the dynamics in the chaotic region. Only in a few cases, it is possible to get an analytical expression for PRD, let us say $\phi(x)$. It is also difficult to get PRD experimentally or numerically, because of the large number of data needed to cover each small subset of length Δx which belongs to the reinjection zone. Because of all this, different approximations have been used in literature to study the intermittency phenomenon.

The most common approximation is to consider PRD uniform, which is independent of the reinjection point [Manneville, 1980; Dubois *et al.*, 1983; Pikovsky, 1983; Kim *et al.*, 1994; Kim *et al.*, 1998; Kim *et al.*, 1997; Cho *et al.*, 2002; Kye *et al.*, 2003; Schuster, 2005]. In different investigations, rather artificial approximations are assumed, and the reinjection is considered in a fixed point [Kim, 1998; Kye & Kim, 2000].

In this research, we present a new one-parameter class of PRDs appearing in many maps with intermittency. For a specific value of the parameter, the new PRDs recover the classical uniform PRD. We also derive the new scaling properties in good agreement with the numerical simulations.

We study a illustrating model

$$x_{n+1} = G(x_n) \equiv \begin{cases} F(x_n) & x_n \le x_r \\ (F(x_n) - 1)^\gamma & x_n > x_r \end{cases} \quad (1)$$

where $F(x) = (1+\epsilon)x_n + (1-\epsilon)x_n^p$, and x_r is the root of the equation $F(x_r) = 1$ (see Fig. 1). The origin $x = 0$ is always a fixed point. It is stable for $\epsilon < 0$. On the contrary, it is unstable for $\epsilon > 0$, and the iterated points x_n of a starting point x_0 close to the origin, increases in a process driven by parameters ϵ and p. When x_n becomes larger than x_r, a chaotic burst occurs that will be interrupted when x_n is again mapped into the laminar region. For $\gamma = 1$ the map (1) can be write as $x_{n+1} = (F(x_n) \mod 1)$ and if in addition, $p = 2$ the map is the same as that used by Manneville in his pioneer paper [Manneville, 1980]. The case $p = 3$ corresponds to the local Poincare map of type-II intermittency for points close to $x = 0$. Note that ϵ and p modified the duration of the mentioned laminar phase, where the dynamics of the system appear periodic and x_n is less than some value, let say c. The function PRD will strongly depend on parameter γ, that determines the curvature of the map in the region around x_r with $x > x_r$. Only points in that region will be mapped inside the laminar region. Note that when γ increases, the number of points also increases that will be mapped around the unstable fixed point $x = 0$.

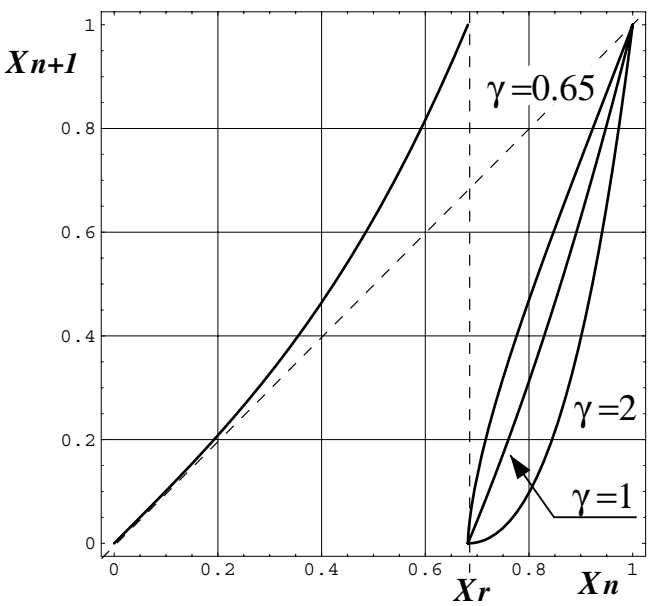

Fig. 1. Map of Eq. (1) with $p = 3$ and $\epsilon = 10^{-3}$. We have used three different values of γ as indicated.

2. Reinjection Probability Distribution

It is clear that PRD is driven by chaotic behavior of the system, and it then depends on the particular systems. In general, it is very difficult to get analytically $\phi(x)$, however, for the map (1) we can used a simple analysis to guess the behavior of $\phi(x)$ near $x = 0$, as the parameter γ changes. To do this, note that all points failing close to the point $x = 0$, emerge from the point close to $x = x_r$, so $\phi(x)$ is connected with the invariant density $\rho(x')$ of the map (1), where x' refers to the preceding interaction, that is, $x' = G_2^{-1}(x)$, where $G_2^{-1}(x)$ is the inverse function of $G(x)$ considering only the definition for $x > x_r$. We need to also rescale $\rho(x')$ to take into account the slope of the function G for points close to x_r and lying on the right side of x_r. Hence, we get for points close to $x = 0$

$$\phi(x) = \rho(x') \frac{K}{\left.\dfrac{\mathrm{d}G(\tau)}{\mathrm{d}\tau}\right|_{\tau=x'}} \quad (2)$$

where K is a normalization constant such that $\int_0^c \phi(\tau)d\tau = 1$.

Note that in Eq. (2), the slope $\lim_{\tau\to x_r^+}(\mathrm{d}G(\tau)/\mathrm{d}\tau)|_{\tau=x'}$ is zero for values of γ higher than 1 and we have $\lim_{\tau\to x_r^+}(\mathrm{d}G(\tau)/\mathrm{d}\tau)|_{\tau=x'} = \infty$ if $\gamma < 1$ (see Fig. 1). Hence, we expect that for $\gamma < 1$ the PRD vanishes near $x = 0$ and, on the other hand, if $\gamma > 1$ we expect $\lim_{x\to 0^+} \phi(x) = \infty$.

In this paper, we do not measure $\phi(x)$ directly from the numerical data. Instead, we use the

function $M(x)$ defined as following

$$M(x) = \frac{\int_0^x \tau\phi(\tau)d\tau}{\int_0^x \phi(\tau)d\tau}. \quad (3)$$

This quantity allows a more reliable experimental and numerical access than $\phi(x)$. Note that for uniform reinjection, we get $M(x) = mx$ with $m = 1/2$. The function (3) is very similar to the function used in [Del Rio *et al.*, 1994] to determine the reinjection probability distribution in the case of type-III intermittency in a electronic circuit. We have numerically evaluated the function $M(x)$ in a broad class of maps obtaining, in good approximation, the lineal form $M(x) = mx$. Similar approximation was found in [Del Rio *et al.*, 1994]. Figure 2 shows numerical evaluations of $M(x)$ for the map (1) using different values of parameter γ together with the corresponding best fit straight line. Note that the slope m can be bigger or less than 1/2 but we always find $|m| < 1$.

According to the previous results, we assume that $M(x) = mx$, so by using Eq. (3), the reinjection probability density reads

$$\phi(x) = bx^\alpha, \quad \text{with } \alpha = -\frac{1-2m}{1-m} \quad (4)$$

where b is determined by the normalization condition

$$\int_0^c bx^\alpha dx = 1 \quad (5)$$

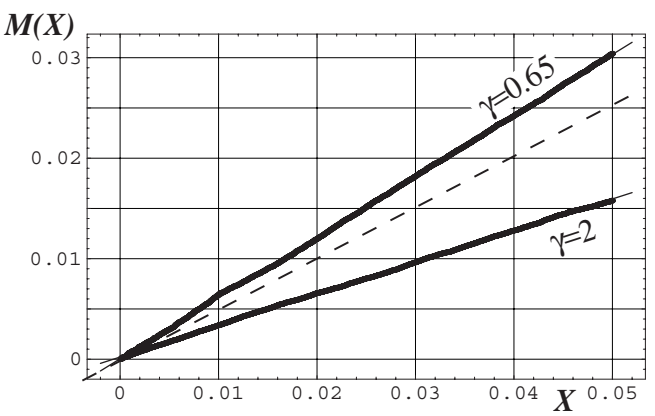

Fig. 2. Function $M(x)$ for the map (1) with $p = 3$. Points correspond to numerical evaluation of $M(x)$ and continuous lines show the cooresponding best lineal fit. The dashed line slope is 0.5 and it corresponds to a uniform reinjection. In the lower line $\gamma = 2$ and $\epsilon = 10^{-3}$ whereas for the upper line $\gamma = 0.65$ and $\epsilon = 10^{-4}$. Numerical evaluation of m yields $m = 0.61$ for upper line and $m = 0.32$ for lower line. The laminar interval is $(0, c)$, with $c = 0.05$.

Assuming $\alpha > -1$, or equivalently $0 < m < 1$, the integral converge and we get

$$b = \frac{\alpha+1}{c^{\alpha+1}} = \frac{m}{1-m}c^{\frac{m}{1-m}} \quad (6)$$

so in the linear approximation $M(x) = mx$, the density $\phi(x)$ is determined only by parameter m, easier to measure than the complete function $\phi(x)$. Note that according to Eq. (4), the behavior of $\phi(x)$ near $x = 0$ can be different for different values of m. That is, we have $\lim_{x\to 0}\phi(x) = \infty$ when m is in the interval $0 < m < 1/2$, whereas $\lim_{x\to 0}\phi(x) = 0$ when m lies in $1/2 < m < 1$ and $\phi(x) = 1/c$ for $m = 1/2$. According to the the previous argument from Eq. (2), we expect for $\gamma > 1$ values of m in the interval $0 < m < 1/2$ and for $\gamma < 1$ values in the interval $1/2 < m < 1$, to be in agreement with data as in Fig. 2. By Eqs. (4) and (6), the value of m is used to determine the PRD, as shown in Fig. 3. In this figure, the numerical reinjection density probabilities are plotted together with the functions $\phi(x)$ for two values of γ used in Fig. 2. Note that we do not fit the numerical data plotted

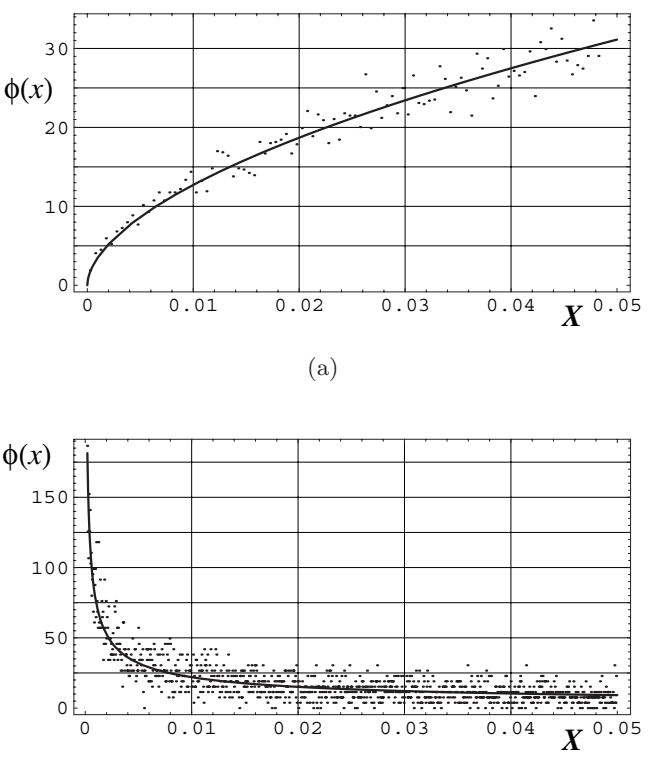

Fig. 3. Reinjection probability density for map (1) using the same parameters as that in Fig. 2. (a) and (b) correspond to the upper and lower lines of Fig. 2 respectively. Dots indicate numerical evaluations and continuous lines show Eq. (4) with the m value being used to plot a continuous line in Fig. 2.

in Fig. 3 but we just plot the function (4) using the value of m calculated to plot continuous lines in Fig. 2.

Note that the expression (4) filters the usual noise of the numerical data, hence it better describes than numerical reinjection density. The same will happen for the length probability density as to be shown below.

3. Characteristic Relations

In the laminar region, we can approximate the difference equation (1) by the differential equation

$$\frac{dx}{dt} = \epsilon x + (1-\epsilon)x^p \tag{7}$$

so the interactions in the laminar region, depending on the reinjection point x is given by

$$l(x,c) = \int_x^c \frac{d\tau}{a\tau^p + \epsilon\tau} \tag{8}$$

where we use the notation $a = 1-\epsilon$. After integration, this yields

$$l(x,c) = \frac{1}{\epsilon}\left[\ln\left(\frac{c}{x}\right) - \frac{1}{p-1}\ln\left(\frac{ac^{(p-1)}+\epsilon}{ax^{(p-1)}+\epsilon}\right)\right]. \tag{9}$$

Note that Eq. (9) refers to a local behavior of the map in the laminar region and it determines the length of laminar period, however, the length statistic of the laminar phases is also affected by the density $\phi(x)$, which is a global property. The probability of finding a laminar phase of length between l and $l+dl$ is $dl\phi_l(l)$, where $\phi_l(l)$ is the duration probability density of the laminar phase. The density $\phi_l(l)$ is related to $\phi(x)$ by $\phi_l(l) = \phi(X(l,c))|(dX(l)/dl)|$, where the function $X(l,c)$ is the inverse function of $l(x,c)$. Hence, by using Eqs. (4) and (9) and after some algebraic manipulation we get

$$\phi_l(l) = b\left(\frac{\epsilon}{\left(a+\frac{\epsilon}{c^{(p-1)}}\right)e^{(p-1)\epsilon l} - a}\right)^{\frac{p+\alpha}{p-1}} \times \left(a+\frac{\epsilon}{c^{(p-1)}}\right)e^{(p-1)\epsilon l} \tag{10}$$

which depends on the global parameter α determined by the slope m of the linear function $M(x)$. Figure 4 shows the analytical expression (10) with the same value of m that we have used in the upper and lower lines of Fig. 2. Also plotted are the corresponding numerical evaluations of ϕ_l.

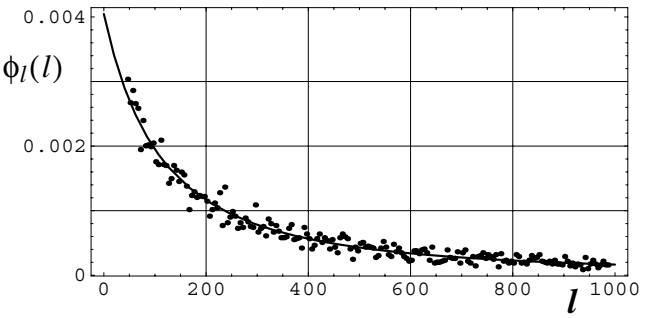

(a)

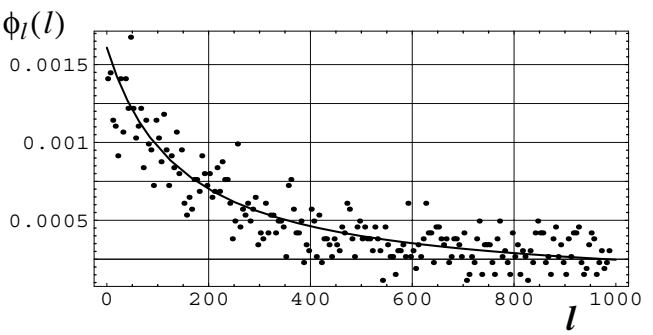

(b)

Fig. 4. Function ϕ_l for the map (1). Two different evaluations: Numerical (dots) and analytical using Eq. (10) (continuous line). The parameters for (a) and (b) are the same as that for the upper and lower lines of Fig. 2, respectively.

Now we consider the average laminar length $\bar{l}$ given by

$$\bar{l} = \int_0^c l(x,c)\phi(x)dx. \tag{11}$$

Then, from Eqs. (4) and (9) and taking into account Eq. (8) we get

$$\bar{l} = \lim_{x\to 0}\frac{b}{\alpha+1}l(x,c)x^{\alpha+1}\Big|_x^c + \frac{b}{\alpha+1}\int_0^c \frac{x^\alpha}{\epsilon + ax^{(p-1)}}dx \tag{12}$$

If $-1 < \alpha$, the limit in Eq. (12) is zero and the second term can be written as

$$\bar{l} = \frac{1}{ac^{\alpha+1}}\left(\frac{a}{\epsilon}\right)^{\frac{p-\alpha-2}{p-1}} \times \left(\int_0^\infty \frac{y^\alpha}{1+y^{(p-1)}}dy - \int_{c_y}^\infty \frac{y^\alpha}{1+y^{(p-1)}}dy\right) \tag{13}$$

where $y = (a/\epsilon)^{1/(p-1)}x$ and $c_y = (a/\epsilon)^{1/(p-1)}c$. The second integral goes to zero as ϵ goes to zero,

whereas the first one, converges in the parameter region $-1 < \alpha < p-2$ or equivalently $0 < m < \frac{p-1}{p}$, so we get for small values of ϵ

$$\bar{l} \approx \frac{1}{ac^{\alpha+1}} \left(\frac{a}{\epsilon}\right)^{\frac{p-\alpha-2}{p-1}} \frac{\pi}{p-1} \sin^{-1}\left(\frac{\pi(1+\alpha)}{p-1}\right). \tag{14}$$

Assuming that α remains constant as ϵ changes, the characteristic relation yields

$$\bar{l} \propto \epsilon^{\beta} \tag{15}$$

where the critical exponent β is given by

$$\beta = \frac{\alpha+2-p}{p-1} = \frac{1+p(m-1)}{(p-1)(1-m)}. \tag{16}$$

Note that β depends on both, the behavior of the local map around the origin (parameter p), and on the global dynamics of reinjection (parameter m). As $-1 < \alpha < p-2$ the critical exponent β can be taken as any value in the interval $(-1, 0)$. Note that the interval for β does not depend on parameter p. We expect that m weakly depends on parameters ϵ and p, hence for several values of γ we evaluate $\bar{l}$ as the values of ϵ change. The results are shown in Fig. 5 for different values of γ and p.

For each point in Fig. 5, the parameter m is evaluated using Eq. (3). It is found that m is approximately independent of γ and p, that is, m can be taken as a constant on each line in Fig. 5, as also shown in Table 1.

Hence, according to the characteristic equation Eq. (15), the expected slope for each lines is β. Note that the slopes can also be evaluated by fitting

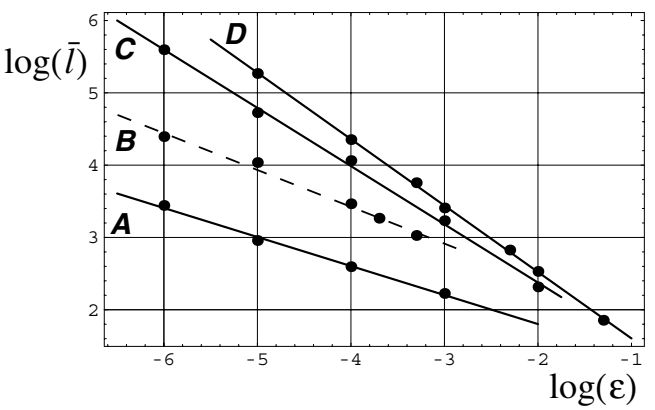

Fig. 5. Characteristic relation for different values of the parameter γ in the map (1). Dots show numerical data and lines show the best fit. For lines B, C and D we used $P = 3$ and the values of γ are 1, 2 and 3 for cases B, C and D, respectively. The value of parameters for line A are $P = 2$ and $\gamma = 1.5$.

Table 1. Parameters γ and p for each line of Fig. 5 and the approximate value of m associated to each line together with the values of α for Eq. (4). Also the corresponding value of the exponent of Eq. (16), the numerical slope of the lines of Fig. 5 and the relative error between both.

	B	A	C	D
p	3	2	3	3
γ	1	1.5	2	3
m	0.49	0.38	0.32	0.22
α from Eq. (4)	−0.02	−0.39	−0.52	−0.72
β from Eq. (16)	−0.51	−0.39	−0.76	−0.86
Numerical slope	−0.51	−0.40	−0.80	−0.92
Relative error	$> 1\%$	3%	5%	7%

against the numerical data in Fig. 5. The results of both methods are very close as shown in Table 1 with the corresponding relative error. Note also that the error between analytical and numerical evaluations increases as the exponent γ increases. This effect can be due to a small nonlinearity observed in the function $M(x)$ as γ goes away from unity.

The particular value $\gamma = 1$ produces uniform reinjection in both cases $p = 3$ and $p = 2$ with $m \approx 0.5$ (see dashed lines in Figs. 5 and 6). Hence for $p = 3$ the map exhibits the classical characteristic relation reported for type-II intermittency $\bar{l} \propto \epsilon^{\frac{1}{2}}$ which is a specific case of Eq. (16) with $p = 3$.

For $\gamma = 1$ and $p = 2$, due to $m \approx 0.5$, we are out of the range of the application of Eq. (14), and also Eq. (16). Note, however that, as $\alpha = 0$ we can evaluate the integral in Eq. (12), getting

$$\bar{l} = \frac{1}{a\,c} \ln\left(\frac{\epsilon + a\,c}{\epsilon}\right) \tag{17}$$

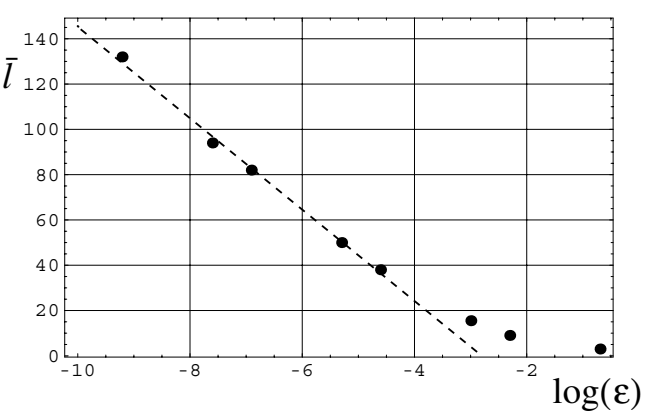

Fig. 6. Characteristic relation for the map (1) with $\gamma = 1$ and $p = 2$. Dashed line fits five points and its slope is approximately -20.2, very close to the expected $-1/c = -20$ for uniform reinjection (see Eq. (18)).

so for small values of ϵ we have

$$\bar{l} \approx \frac{1}{c} (\ln c - \ln \epsilon) \tag{18}$$

as shown in Fig. 6.

4. Conclusion and Discusion

We present the function (3) as a tool to determine the reinjection probability density $\phi(x)$. The quantity $M(x)$ has a more reliable numerical and experimental access than $\phi(x)$. In a number of cases $M(x) \approx mx$, then we have $\phi(x) = bx^{\alpha}$. This is a generalization of the usual uniform reinjection approximation which correspond to $\alpha = 0$ or $m = 1/2$. The analytical expression is derived for duration probability density of the laminar phase $\phi_l(l)$ according to the new PRD. Also a general characteristic relation for type-II intermittency, is derived e^{β} with $-1 < \beta < 0$. The critical exponent β is determined, through Eq. (16), by quantity m. All results are compared with numerical simulations finding good agreement with the analytical predictions.

As the reinjection mechanism around an unstable point is a global property, independent of the local instability of the map, we can study the reinjection probability density in a map without intermittency. Hence, to illustrate how a nonlinear mechanism of reinjection can change the PRD, from uniform reinjection (map (1) with $\gamma = 1$) to the expression $\phi(x) = bx^{\alpha}$ (map (1) with $\gamma \neq 1$), we consider the well-known tent map defined as $X_{n+1} = T_1(x_n)$ where

$$T_1(x) = \begin{cases} 2x & x \leq \dfrac{1}{2} \\ 2 - 2x & x > \dfrac{1}{2} \end{cases}. \tag{19}$$

Let be $H(x) = x^q$ for $q > 0$ and let T_q be defined by the composition of function

$$T_q \equiv H \circ T_1 \circ H^{-1} = \begin{cases} 2^q x & x \leq \dfrac{1}{2^q} \\ (2 - 2x^{1/q})^q & x > \dfrac{1}{2^q} \end{cases} \tag{20}$$

and we consider the following map $x_{n+1} = T_q(x_n)$ (see Fig. 7).

Note that, due to T_q being a topologically conjugate map of the tent map, in the sense used by Hao [1989], its invariant density $\rho_q(x)$ is related to the invariant density $\rho_1(x)$ of the tent map by

$$\rho_p(x) = \rho_1(H^{-1}(x)) \left| \frac{\mathrm{d}H^{-1}}{\mathrm{d}x} \right|. \tag{21}$$

Since $\rho_1(x) = 1$, we have

$$\rho_q(x) = \frac{x^{\frac{1}{q}-1}}{q}. \tag{22}$$

then, after applying Eq. (2) to the function T_q, we get for the PRD of the map $X_{n+1} = T_q(x_n)$, the expression $\phi_q(x) = bx^{\alpha}$ where

$$\alpha = \frac{1}{q-1} \tag{23}$$

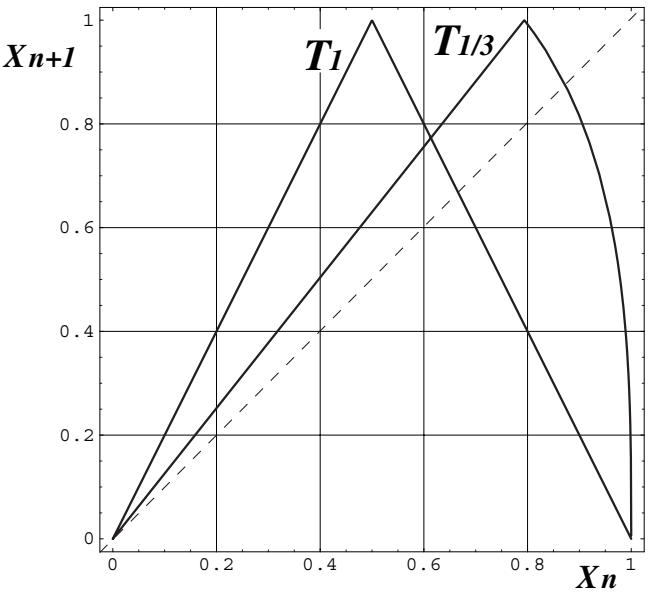

Fig. 7. Two maps T_q for $q = 1, 1/3$. Tent map is labeled by T_1.

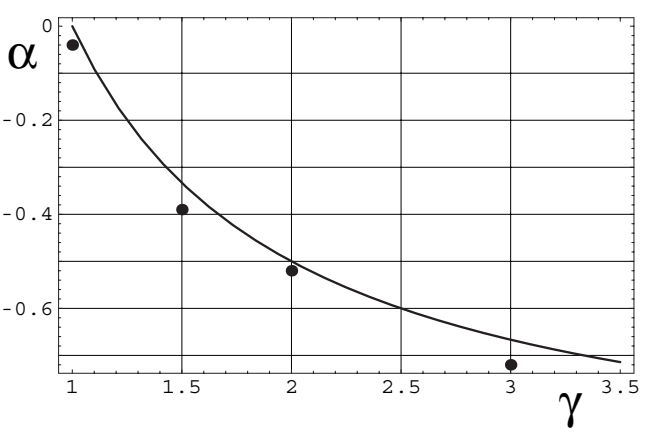

Fig. 8. Exponent α as a function of γ. Dots show the values of Table 1 whereas in a continuous line is plotted Eq. (23) with the identification $q = \gamma$.

that is, Eq. (4) is an exact result for $X_{n+1} = T_q(x_n)$, then, we have the next exact result for $M(x)$

$$M(x) = \frac{1}{1+q}x. \tag{24}$$

In this example, Eq. (4) appears as a natural generalization ($q \neq 1$) of the uniform reinjection ($q = 1$). It seems to be a similar mechanism for the map (1), as it is suggested by comparison between both maps. In fact, the parameter γ in the map (1) and q in $x_{n+1} = T_q(x_n)$ play a simillar roll in the sense that for $q = \gamma = 1$ we have uniform reinjection in both cases. Moreover, as seen in Fig. 8, we can substitute in Eq. (23) q by γ to get approximated values of exponent α for the PRD of the map (1).

Acknowledgments

This research was supported by Technical University of Madrid under grant AL09-PID-03 and by CONICET under grant PID-5269, Universidad Nacional de Cordoba and Ministerio de Ciencia y Tecnologia de Cordoba.

References

Cho, J.-H., Ko, M.-S., Park, Y.-J. & Kim, C.-M. [2002] "Experimental observation of the characteristic relations of type-I intermittency in the presence of noise," *Phys. Rev. E* **65**, 036222.

Crutchfield, J. D., Farmer, J. P. & Huberman, B. A. [1982] "Fluctuations and simple chaotic dynamics," *Phys. Rep.* **92**, 45–82.

Del Rio, E., Velarde, M. G. & Rodriguez-Lozano, A. [1994] "Long time data series and diffuculties with the characterization of chaotic attractors: A case with intermittency III," *Chaos Solit. Fract.* **4**, 2169–2179.

Dubois, R. M. A. & Berg, P. [1983] "Experimental evidence of intermittencies associated with a subharmonic bifurcation," *Phys. Rev. Lett.* **51**, 1446–1449.

Grebogi, C., Ott, E., Romeiras, F. & Yorke, J. A. [1987] "Critical exponents for crisis induced intermittency," *Phys. Rev. A* **36**, 5365–5380.

Hao, B.-L. [1989] *Elementary Symbolic Dynamics and Chaos in Dissipatice Systems* (World Scientific Publishing, Singapore), Chap. 2, pp. 53–55.

Kim, C.-M., Kwon, O.J., Lee, E.-K. & Lee, H. [1994] "New characteristic relations in type-I intermittency," *Phys. Rev. Lett.* **73**, 525–528.

Kim, C.-M., Yim, G.-S., Kim, Y. S., Kim, J.-M. & Lee, H. W. [1997] "Experimental evidence of characteristic relations of type-I intermittency in an electronic circuit," *Phys. Rev. E* **56**, 2573–2577.

Kim, C.-M., Yim, G.-S., Ryu, J.-W. & Park, Y.-J. [1998] "Characteristic relations of type-III intermittency in an electronic circuit," *Phys. Rev. Lett.* **80**, 5317–5320.

Kye, W.-H. & Kim, C.-M. [2000] "Characteristic relations of type-I intermittency in the presence of noise," *Phys. Rev. E* **62**, 6304–6307.

Kye, W.-H., Rim, S. & Kim, C.-M. [2003] "Experimental observation of characteristic relations of type-III intermittency in the presence of noise in a simple electronic circuit," *Phys. Rev. E* **68**, 036203.

Manneville, P. & Pomeau, Y. [1979] "Intermittency and Lorenz model," *Phys. Lett. A* **75**, 1–2.

Manneville, P. [1980] "Intermittency, self-similarity & 1/f spectrum in dissipative dynamical systems," *Le Journal de Physique* **41**, 1235–1243.

Ott, E. [1993] *Chaos in Dynamical Systems* (Cambridge University Press, Cambridge), Chap. 8, pp. 310–315.

Pikovsky, A. S. [1983] "A new type of intermittent transition to chaos," *J. Phys. A* **16**, L109–L112.

Pomeau, Y. & Manneville, P. [1980] "Intermittent transitions to turbulence in dissipative dynamical systems," *Commun. Math. Phys.* **74**, 189–197.

Schuster, H. G. & Just, W. [2005] *Deterministic Chaos* (Wiley-VCH Verlag GmbH & Co. KGaA, Federal Republic of Germany), Chap. 5, pp. 59–88.

Stavrinides, S. G., Miliou, A. N., Laopoulos, Th. & Anagnostopoulos, A. N. [2008] "The intermittency route to chaos of an electronic digital oscillator," *Int. J. Bifurcation and Chaos* **18**, 1561–1566.

Zebrowski, J. J. & Baranowski, R. [2004] "Type I intermittency in nonstationary systems: Models and human heart-rate variability," *Physica A* **336**, 7483.